

## Electronic Supplementary Information

### Time-Resolved Fluorescence Anisotropy as a Tool to Study Guest-Cucurbit[n]uril-Protein Ternary Supramolecular Interactions

Karina Scholtbach,<sup>a</sup> Ítalo Venegas,<sup>a</sup> Cornelia Bohne<sup>b</sup> and Denis Fuentelba<sup>a\*</sup>

<sup>a</sup> Laboratorio de Química Biológica, Departamento de Química Física, Facultad de Química, Pontificia Universidad Católica de Chile, Santiago, Chile. Corresponding author: Denis Fuentelba (dlfuentelba@uc.cl)

<sup>b</sup> Department of Chemistry, University of Victoria, P.O. Box 3065, Victoria, BC, Canada V8W 3V6.

#### Index

1. Numerical analysis for the determination of binding constants	S2
2. Correction of the fluorescence intensity for the inner-filter effect	S2
3. Binding of Trp-Gly-Gly to CB[8] (figure S1)	S2/3
4. Binding of AO <sup>+</sup> to HSA determined by fluorescence quenching (figure S2)	S3
5. Binding isotherm for AO <sup>+</sup> with HSA (figure S3)	S3
6. Fluorescence decays for AO <sup>+</sup> free and bound to CB[7] or CB[8] (figure S4)	S3
7. Fluorescence anisotropy analysis for AO <sup>+</sup> @CB[7] complex in the presence of HSA	S3
8. Simulation of the anisotropy decays for the formation of the species AO <sup>+</sup> :HSA and AO <sup>+</sup> @CB[7]:HSA (figure S5)	S3/4
9. Fluorescence anisotropy analysis for AO <sup>+</sup> @CB[8] complex in the presence of HSA (figures S6 and S7)	S4
10. Quenching of HSA fluorescence by AO <sup>+</sup> @CB[7] complex and AO <sup>+</sup> (figure S8 and table S1)	S5
11. References	S5

## 1. Numerical analysis for the determination of binding constants

Numerical analysis of the experimental data was carried out using Scientist 3.0 software from Micromath. The mathematical models for the 1:1 binding of 2-naphthyl-1-ethylammonium to CB[7] were reported previously.<sup>1</sup> In the present work, the overall binding constant for the 1:1 complex ( $\beta_{11}$ ) was obtained by fitting the fluorescence intensity increase for an  $\text{AO}^+$  solution in the presence of different concentrations of CB[7] according to eq. S1-S4 (overall binding constants  $\beta$  are bold to differentiate them from  $\beta$  values in the anisotropy analysis). It must be noted that the concentration of guest free CB[7] ( $[\text{CB}[7]]_{\text{GF}}$ ) corresponds to the sum of free CB[7],  $\text{Na}^+\cdot\text{CB}[7]$  and  $\text{Na}^+\cdot\text{CB}[7]\cdot\text{Na}^+$ .<sup>1</sup>  $I_0$  and  $I$  correspond to the fluorescence intensities in the absence and presence of CB[7], respectively. The intensities for  $\text{AO}^+$  were normalized to unity for solutions in the absence of CB[7] to account for fluctuations of the excitation intensities of the fluorimeter on different days. This normalization factor was used for all other intensities. The parameter  $C_{11}$  corresponds to the ratio between the emission quantum efficiencies for the CB[7] complex and free  $\text{AO}^+$  and the value for this parameter was  $9 \pm 2$ .

$$I = \frac{I_0}{[\text{AO}^+]_{\text{total}}} \times ([\text{AO}^+] + C_{11} \times [\text{AO}^+@CB[7]]) \quad (\text{S1})$$

$$\beta_{11} = \frac{[\text{AO}^+@CB[7]]}{[\text{AO}^+][\text{CB}[7]]_{\text{GF}}} \quad (\text{S2})$$

$$[\text{AO}^+]_{\text{total}} = [\text{AO}^+] + [\text{AO}^+@CB[7]] \quad (\text{S3})$$

$$[\text{CB}[7]]_{\text{total}} = [\text{CB}[7]]_{\text{GF}} + [\text{AO}^+@CB[7]] \quad (\text{S4})$$

Similarly, the overall binding constants for the 1:1 ( $\beta_{11}'$ ) and 2:1 ( $\beta_{21}$ ) complexes with CB[8] were determined by fitting the fluorescence intensity decrease for an  $\text{AO}^+$  solution in the presence of different concentrations of CB[8] according to eq. S5-S9. The parameters  $C_{11}'$  and  $C_{21}$  correspond to the ratios between the emission quantum efficiencies for the 1:1 or 2:1 complexes with CB[8] and free  $\text{AO}^+$ . The value recovered for  $C_{11}'$  was  $0.022 \pm 0.001$ . The value estimated for  $C_{21}$  was  $1.9 \pm 0.1$  using a 5-fold excess of  $\text{AO}^+$  over CB[8] as stated in the paper.

$$I = \frac{I_0}{[\text{AO}^+]_{\text{total}}} \times \left( [\text{AO}^+] + C_{11}' \times [\text{AO}^+@CB[8]] + \frac{C_{21} \times [\text{AO}^+_2@CB[8]]}{[\text{AO}^+]} \right) \quad (\text{S5})$$

$$\beta_{11}' = \frac{[\text{AO}^+@CB[8]]}{[\text{AO}^+][\text{CB}[8]]_{\text{GF}}} \quad (\text{S6})$$

$$\beta_{21} = \frac{[\text{AO}^+_2@CB[8]]}{[\text{AO}^+][\text{AO}^+@CB[8]]} \quad (\text{S7})$$

$$[\text{AO}^+]_{\text{total}} = [\text{AO}^+] + [\text{AO}^+@CB[8]] + 2[\text{AO}^+_2@CB[8]] \quad (\text{S8})$$

$$[\text{CB}[8]]_{\text{total}} = [\text{CB}[8]]_{\text{GF}} + [\text{AO}^+@CB[8]] + [\text{AO}^+_2@CB[8]] \quad (\text{S9})$$

## 2. Correction of the fluorescence intensity for the inner-filter effect

The emission intensities were corrected to account for the inner-filter effect due to the presence of  $\text{AO}^+$ , which absorbs at the excitation and emission wavelengths. For this purpose we used eq. S10, which takes into account the absorbance of the added  $\text{AO}^+$  at the excitation ( $A_{\text{ex}}$ ) and emission ( $A_{\text{em}}$ ) wavelengths. This equation assumes self-absorption is negligible, the fluorescence quantum yield is independent of the excitation wavelength and the emission is centered on the fluorescence cell.<sup>3</sup> We tested the applicability of the inner-filter correction factor to our system by determining the Stern-Volmer constant for 1-naphthyl-1-ethanol quenched by sodium iodide,<sup>4</sup> in the presence of increasing concentrations of  $\text{AO}^+$ . The recovered quenching constant in the presence of  $\text{AO}^+$  was accurate within 10% error.

$$I_{\text{corrected}} = I \times 10^{0.5(A_{\text{ex}}+A_{\text{em}})} \quad (\text{S10})$$

## 3. Binding of Trp-Gly-Gly to CB[8] as a control system

Trp-Gly-Gly forms a 2:1 inclusion complex with CB[8], with a reported binding constant of  $1.3 \times 10^5 \text{ M}^{-1}$  for the binding of the first Trp-Gly-Gly to CB[8] and a binding constant of  $2.8 \times 10^4 \text{ M}^{-1}$  for the inclusion of the second molecule determined by ITC in 10 mM phosphate buffer pH 7.0 at 27°C.<sup>2</sup> In the present work, the binding of Trp-Gly-Gly to CB[8] was followed by the decrease in the fluorescence intensity of the tripeptide at 360 nm (Fig. S1). It is worth noting that CB[8] does not have significant absorption at this wavelength (absorbance increase  $\leq 0.01$ ). The parameter  $C_{21}$  was estimated to be 1.8 in a similar manner as the value determined for  $\text{AO}^+$  with CB[8] in the paper and it was fixed for the numerical analysis. The parameter  $C_{11}$  was recovered from the fits and it was equal to  $0.14 \pm 0.03$ . The stepwise binding constants obtained for this system were  $(1.4 \pm 0.6) \times 10^6 \text{ M}^{-1}$  and  $(3 \pm 1) \times 10^5 \text{ M}^{-1}$  for the first and second steps, respectively.

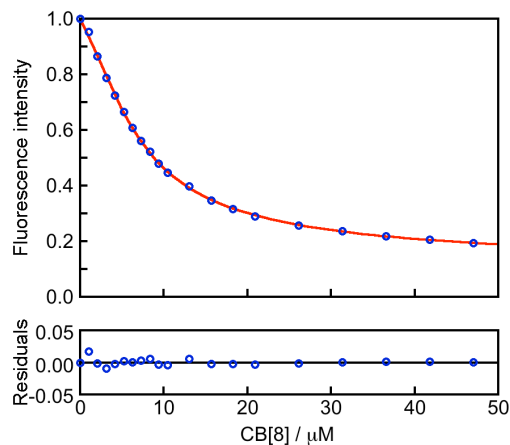


**Figure S1.** Fluorescence intensity for a 6  $\mu\text{M}$  Trp-Gly-Gly solution in the presence of different concentrations of CB[8] in 10 mM phosphate buffer pH 7.0 at 27 °C. The data were fit in an analogous manner to eq. S5-S9.

The binding constants determined by fluorescence titration are one order of magnitude higher than the values determined by ITC reported previously, and this difference is likely experimental. It is important to note that we were interested in the ratios as mentioned in the paper.

#### 4. Binding of $\text{AO}^+$ to HSA determined by fluorescence quenching

The quenching plot for HSA in the presence of  $\text{AO}^+$  is shown on figure S2. The binding constant obtained from the Stern-Volmer plot was  $(2.5 \pm 0.4) \times 10^4 \text{ M}^{-1}$ .

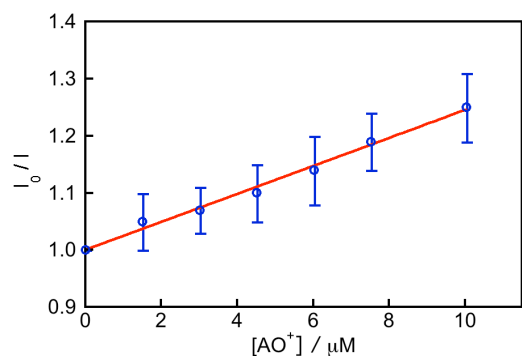


**Figure S2.** Stern-Volmer plot for HSA (5 μM) quenched with  $\text{AO}^+$  in 10 mM phosphate buffer pH 7.0 at 20 °C. The samples were excited at 280 nm and the emission was collected at 340 nm.

#### 5. Binding isotherm for $\text{AO}^+$ with HSA

The binding of  $\text{AO}^+$  to HSA was examined by following the increase in the fluorescence when exciting the samples at 420 nm and measuring the emission intensity at 530 nm (Fig. S3). The data fit well to a 1:1 model using a similar approach as the binding of  $\text{AO}^+$  to CB[7] (eq. S1-S4). The increment in the efficiency for the fluorescence emission for the  $\text{AO}^+$ :HSA complex was  $1.6 \pm 0.1$  and the binding constant was  $(2.0 \pm 0.5) \times 10^5 \text{ M}^{-1}$ . This value must be considered at best an overall binding affinity since the difference with the value obtained from the quenching studies suggests that binding to multiple sites occurs.

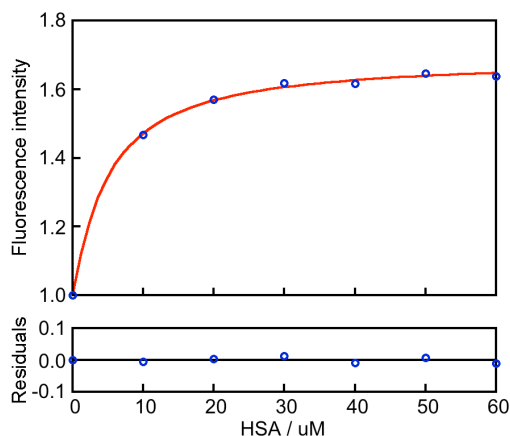


**Figure S3.** Fluorescence intensity for  $\text{AO}^+$  (2 μM) in the presence of different concentrations of HSA in 10 mM phosphate buffer pH 7.0 at 20 °C. The data were fit in an analogous manner to eq. S1-S4.

#### 6. Fluorescence decays for $\text{AO}^+$ free and bound to CB[7] or CB[8]

The fluorescence decays for  $\text{AO}^+$  free in solution,  $\text{AO}^+$ @CB[7] complex and  $\text{AO}^+$ @CB[8] complex are shown on figure S4. The fluorescence decay becomes slower (longer lifetime) when  $\text{AO}^+$  forms inclusion complexes with CB[7] and CB[8]. It must be noted that fluorescence decays for lifetimes determinations were obtained by collecting a minimum of 2000 counts and the results were the same at 10000 counts.

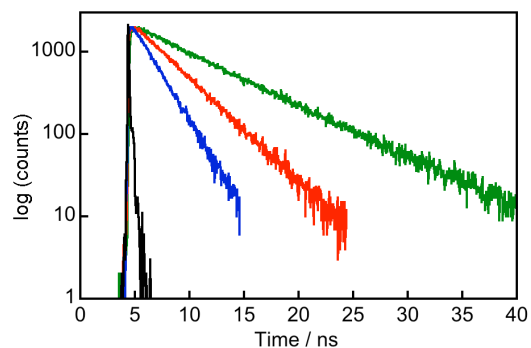


**Figure S4.** Fluorescence decay for  $\text{AO}^+$  (2 μM) in the absence (blue) and presence of 50 μM CB[7] (red) or 20 μM CB[8] (green) in 10 mM phosphate buffer pH 7.0 at 20 °C.

#### 7. Fluorescence anisotropy analysis for $\text{AO}^+$ @CB[7] complex in the presence of HSA

When the anisotropy decay for an  $[\text{AO}^+\text{@CB[7]}]/[\text{HSA}]$  ratio of 0.2 was fit using numerical analysis without fixing the values of the rotational correlation times, only the  $r_0$  value and the shorter rotational correlation time were recovered. The other rotational correlation time did not converge into a single value because its contribution to the intensity of the anisotropy decay was too small and its anisotropy decay was too long compared to the time scale for the measurement. Fixing a large range of values between 30 ns and 100 ns for the longer rotational correlation time gave acceptable fits without affecting the value of 0.44 ns for the other rotational correlation time or the value of 0.33 for  $r_0$ . In a previous work a value of  $55 \pm 5$  ns was recovered for HSA-bound anthracene carboxylate,<sup>5</sup> and this value was in agreement with previous literature reports. Therefore, in the present work we fixed the long rotational correlation time to 55 ns for the analysis. The important point for the objective of identifying a new emitting species in this work was not the absolute value of the long rotational correlation time, but it was establishing the existence of this species.

#### 8. Simulation of the anisotropy decays for the formation of the species $\text{AO}^+$ :HSA and $\text{AO}^+$ @CB[7]:HSA

Only one fluorescence lifetime was observed for the mixture of  $\text{AO}^+$ @CB[7] with HSA, which lengthened at increasing concentration ratios. Since the  $\text{AO}^+$ :HSA complex has a long fluorescence lifetime, we needed to discard the possibility that the lengthening observed was due to the displacement of  $\text{AO}^+$  from the complex with CB[7] into HSA. The presence

of both species could give an "average lifetime" (amplitude-weighted lifetime) that was longer if the contribution of one of the species is small. The fluorescence lifetimes of  $\text{AO}^+\text{@CB}[7]$  and  $\text{AO}^+\text{:HSA}$  were known to be 3.46 ns and 4.77 ns, respectively. Therefore, we calculated the  $A$  values that would mathematically give us the average lifetime observed for the samples using eq. S11 and knowing that the sum of  $A$  values is unity.

$$\langle \tau \rangle = \sum_i A_i \tau_i \quad (\text{S11})$$

The  $A$  values obtained for the  $\text{AO}^+\text{:HSA}$  species were 0.008, 0.038, 0.069, 0.145, 0.160 and 0.221 for  $[\text{AO}^+\text{@CB}[7]]/[\text{HSA}]$  ratios of 0.2, 1, 2, 3, 4 and 5, respectively. Such large  $A$  values are in principle separable from the contribution of the  $\text{AO}^+\text{@CB}[7]$  complex in the time-resolved fluorescence experiment. Therefore, if displacement was occurring the two species would have been detected. Nevertheless, we simulated the anisotropy decays using the associated model (eq. 4-6 in the paper) with the calculated  $A$  values for each concentration ratio, and knowing the fluorescence lifetimes and rotational correlation times for  $\text{AO}^+\text{@CB}[7]$  and  $\text{AO}^+\text{:HSA}$  (0.39 ns and 55 ns, respectively). The simulated anisotropy decays (Fig. S5) show that a growth would be observed if the  $\text{AO}^+\text{:HSA}$  complex was present.

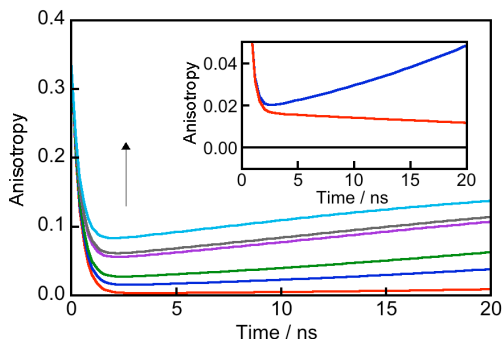


**Figure S5.** Simulation of the fluorescence anisotropy decay for a mixture of the species  $\text{AO}^+\text{:HSA}$  and  $\text{AO}^+\text{@CB}[7]$  at different concentration ratios of  $\text{AO}^+\text{@CB}[7]/\text{HSA}$ . The arrow indicates increasing concentration ratios of 0.2, 1, 2, 3, 4 and 5. Inset: Comparison between the simulation of the anisotropy decay for a ratio of  $[\text{AO}^+\text{@CB}[7]]/[\text{HSA}]$  of 1 for a mixture of the species  $\text{AO}^+\text{:HSA}$  and  $\text{AO}^+\text{@CB}[7]$  (blue), and the simulation of a mixture of the species  $\text{AO}^+\text{@CB}[7]$  and  $\text{AO}^+\text{@CB}[7]\text{:HSA}$  (red) under the same conditions.

### 9. Fluorescence anisotropy analysis for $\text{AO}^+_2\text{@CB}[8]$ complex in the presence of HSA

The anisotropy decays for  $\text{AO}^+_2\text{@CB}[8]$  complex in the presence of HSA are shown on figure S6.

Notice that for the samples in the presence of CB[8] the residuals for the fit are not completely random around zero at short time windows. The rotational correlation times obtained for these fits (see  $\phi_2$  in table 3 in the paper) were slightly shorter than the value obtained in the absence of HSA ( $0.63 \pm 0.03$  ns). This is likely an artifact related to the aggregation of HSA in the presence of CB[8], which could scatter some light in the solution, as reported for BSA.<sup>6</sup> Fast

decaying components can be associated to scattered light reaching the detector, while emitted photons can be scattered before they are detected giving rise to lower anisotropy values.<sup>7</sup> The shorter rotational correlation times and the lower  $r_0$  values observed for the samples in the presence of HSA suggest the aggregation of the protein to some extent.

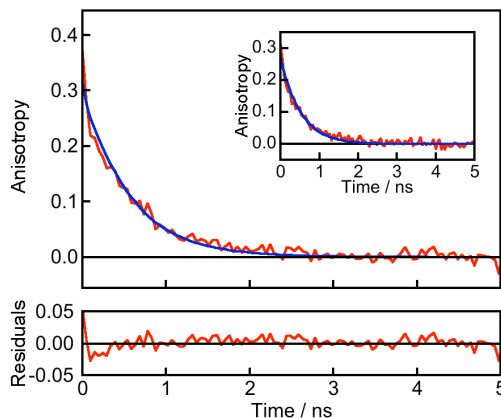


**Figure S6.** Fluorescence anisotropy decay for  $\text{AO}^+_2\text{@CB}[8]$  complex in the presence of HSA at an  $[\text{AO}^+]_{\text{total}}/[\text{HSA}]$  ratio of 1. Inset: Data for an  $[\text{AO}^+]_{\text{total}}/[\text{HSA}]$  ratio of 4. All samples in 10 mM phosphate buffer pH 7.0 at 20 °C. The data was fit to eq. 4-6 in the paper using  $i=2$  and  $j=2$ .

If the data were fit using three rotational correlation times instead of two, the residuals were random around zero (Fig. S7). For this fit, an additional short rotational correlation time ( $< 0.07$  ns) could be detected, which is too short to correspond to the rotation of any  $\text{AO}^+$  species, and is close to the time resolution of the system, which is consistent with light scattering. For this fit, the rotational correlation time corresponding to the species with a fluorescence lifetime of 6.91 ns was  $0.64 \pm 0.05$  ns, in good agreement with the value observed in the absence of HSA.

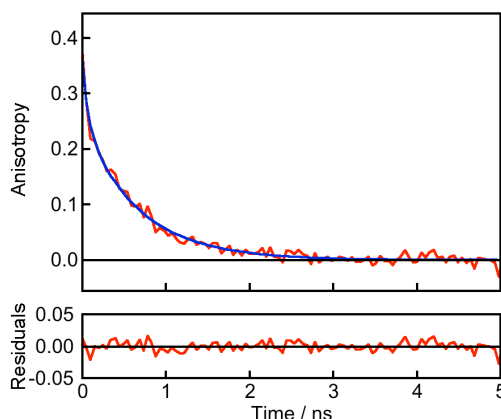


**Figure S7.** Refit of data in figure S6 for  $\text{AO}^+_2\text{@CB}[8]$  complex in the presence of HSA at an  $[\text{AO}^+]_{\text{total}}/[\text{HSA}]$  ratio of 1 in 10 mM phosphate buffer pH 7.0 at 20 °C. The data were fit to eq. 4-6 in the paper using  $i=2$  and  $j=3$ .

## 10. Quenching of HSA fluorescence by $\text{AO}^+\text{@CB[7]}$ complex and $\text{AO}^+$

The HSA fluorescence intensity decreased after the addition of  $\text{AO}^+\text{@CB[7]}$  complex to the solution (Fig. S8). This intensity decrease is due to two main factors: the partial absorption of the excitation light at 280 nm by  $\text{AO}^+$  and the quenching of the singlet excited state of HSA. Therefore, the magnitude of the decrease does not correlate with the quenching unless the intensities are corrected by the absorption of  $\text{AO}^+$ , as indicated above. Distortions in the shape of the spectra might arise due to reabsorption of the emitted light by  $\text{AO}^+$ .

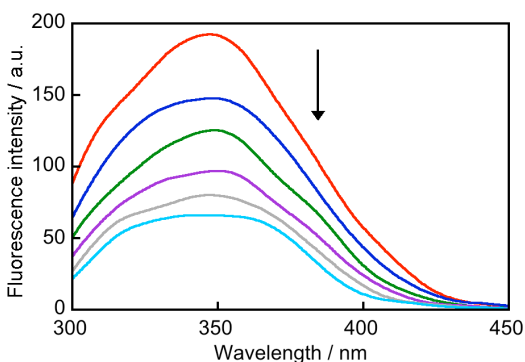


**Figure S8.** Fluorescence spectra for HSA (5  $\mu\text{M}$ ) quenched with  $\text{AO}^+\text{@CB[7]}$  complex in 10 mM phosphate buffer pH 7.0 at 20  $^\circ\text{C}$ . The samples were excited at 280 nm.

The fluorescence lifetimes for HSA in the presence of different concentrations of  $\text{AO}^+\text{@CB[7]}$  are shown in table S1. It is important to note that the HSA fluorescence lifetimes did not change with the addition of  $\text{AO}^+\text{@CB[7]}$ , but the intensity decreased as shown above.

**Table S1.** Fluorescence lifetimes and pre-exponential factors for HSA (5  $\mu\text{M}$ ) in the presence of different concentrations of  $\text{AO}^+\text{@CB[7]}$  in 10 mM phosphate buffer pH 7.0 at 20  $^\circ\text{C}$ .<sup>a</sup>

$[\text{AO}^+\text{@CB[7]}] / \mu\text{M}$	$\tau_1 / \text{ns} (A_1)$	$\tau_2 / \text{ns} (A_2)$
<sup>b</sup> -	3.23 (0.26)	7.50 (0.74)
5	3.38 (0.27)	7.47 (0.73)
10	3.14 (0.25)	7.43 (0.75)
15	3.33 (0.27)	7.44 (0.73)
20	3.22 (0.29)	7.50 (0.71)
25	3.28 (0.28)	7.51 (0.72)

<sup>a</sup>The ratio between CB[7] and HSA was kept fixed at 10:1 to ensure the binding of  $\text{AO}^+$  to CB[7]. <sup>b</sup>HSA in the absence of  $\text{AO}^+$  and CB[7].

## 11. References

1. H. Tang, D. Fuentealba, Y. H. Ko, N. Selvapalam, K. Kim and C. Bohne, Guest Binding Dynamics with Cucurbit[7]uril in the Presence of Cations, *J. Am. Chem. Soc.*, 2011, **133**, 20623–20633.
2. L. M. Heitmann, A. B. Taylor, P. J. Hart and A. R. Urbach, Sequence-Specific Recognition and Cooperative Dimerization of N-Terminal Aromatic Peptides in Aqueous Solution by a Synthetic Host, *J. Am. Chem. Soc.*, 2006, **128**, 12574-12581.
3. R. A. Leese and E. L. Wehry, Corrections for Inner-Filter Effects in Fluorescence Quenching Measurements via Right-Angle and Front-Surface Illumination, *Anal. Chem.*, 1978, **50**, 1193-1197.

4. R. Li, E. Carpentier, E. D. Newell, L. M. Olague, E. Heafey, C. Yihwa and C. Bohne, Effect of the Structure of Bile Salt Aggregates on the Binding of Aromatic Guests and the Accessibility of Anions, *Langmuir*, 2009, **25**, 13800-13808.
5. D. Fuentealba, H. Kato, M. Nishijima, G. Fukuhara, T. Mori, Y. Inoue and C. Bohne, Explaining the Highly Enantiomeric Photocyclodimerization of 2-Anthracenecarboxylate Bound to Human Serum Albumin Using Time-Resolved Anisotropy Studies, *J. Am. Chem. Soc.*, 2013, **135**, 203-209.
6. W. Lei, G. Jiang, Q. Zhou, B. Zhang and X. Wang, Greatly Enhanced Binding of a Cationic Porphyrin Towards Bovine Serum Albumin by Cucurbit[8]uril, *Phys. Chem. Chem. Phys.*, 2010, **12**, 13255-13260.
7. J. R. Lakowicz, *Principles of Fluorescence Spectroscopy*, Springer, New York, 4th edn., 2006.